



Power Electronic Systems
Laboratory

© 2015 IEEE

Proceedings of the 17th European Conference on Power Electronics and Applications (ECCE Europe 2015), Geneva, Switzerland, September 8-10, 2015

Fast Method for the Calculation of Power Losses in Foil Windings

I. Kovacevic-Badstübner,
R. Burkart,
C. Dittli,
A. Müsing,
J. W. Kolar

This material is published in order to provide access to research results of the Power Electronic Systems Laboratory / D-ITET / ETH Zurich. Internal or personal use of this material is permitted. However, permission to reprint/republish this material for advertising or promotional purposes or for creating new collective works for resale or redistribution must be obtained from the copyright holder. By choosing to view this document, you agree to all provisions of the copyright laws protecting it.



Eidgenössische Technische Hochschule Zürich
Swiss Federal Institute of Technology Zurich

A Fast Method for the Calculation of Foil Winding Losses

Ivana Kovačević-Badstübner, Ralph Burkart, Cédric Dittli
and Johann W. Kolar
Power Electronic Systems Laboratory
ETH Zürich, Physikstrasse 3
CH-8092 Zürich, Switzerland
Phone: +41 44 632 28 33
www.pes.ee.ethz.ch

Andreas Müsing
GECKO-SIMULATIONS AG
Physikstrasse 3, ETL H13
CH-8092 Zürich, Switzerland
Phone: +41 44 632 42 65
Fax: +41 44 632 12 12
www.gecko-simulations.com

Keywords

«Magnetic device», «Modeling», «Design», «Estimation Technique».

Abstract

This paper introduces a new two-dimensional (2D) modeling approach for the fast calculation of inductor and transformer foil winding losses. The proposed modeling procedure is derived from the Partial Element Equivalent Circuit (PEEC) method, which is originally a full three-dimensional (3D) electromagnetic solution technique. With the presented modifications, the PEEC method can take into account the influence of an air gap fringing field and core material boundaries as well as skin- and proximity effect. A comparison to 2D Finite Element Method (FEM) simulations shows that the developed PEEC-based approach exhibits similar accuracy but shorter calculation times than the classical FEM modeling techniques typically employed for the calculation of non-uniform current distribution within foil windings. The new modeling approach is experimentally verified by calorimetric loss measurements of a gapped foil winding E-core inductor. Due to the fast calculation speed of the new approach, optimizations of inductive components with foil windings over a wide design space are finally possible.

Introduction

The recent development of power power electronic converters is mainly focused towards higher energy efficiency and higher power density at lower costs and reduced R&D time. A major requirement for achieving these targets is the optimization of magnetic components. CAD tools based on the Finite Element Method (FEM) have so far been used for loss calculation of power inductors and transformers. However, the model set-up and parametrization effort of valid FEM models is a time-consuming task. Additionally, FEM is not the best choice for a fast calculation over a design space of hundreds of different samples. The calculation time for a sample should be in the range of a few seconds in order to allow the examination of many different designs within a reasonable time.

Depending on the application, an optimized design choice for inductors and transformers is performed in the direction of minimizing the volume, total loss of the component, or unit cost. Understanding and control of the generation of heat dissipation is, however, always of major importance. The total losses of magnetic components can be subdivided into core losses and winding losses. A novel approach for the calculation of the core losses taking into account non-sinusoidal current waveforms and the DC magnetization field (H_{DC}) was presented in [1]. In this paper, [1] will be extended with a fast and accurate calculation of foil winding losses. The attractiveness of the proposed electromagnetic modeling method is based on its straightforward mathematical principle; only a small set of simple equations is required. This enables the reader to easily reproduce the approach in any computation environment as e.g. Matlab. The origin of high frequency winding losses in magnetic components is due to eddy currents produced by magnetic fields, which are in turn generated by alternating currents of conductors or other external field sources such as the air gap fringing field. The alternating conductor current produces a magnetic

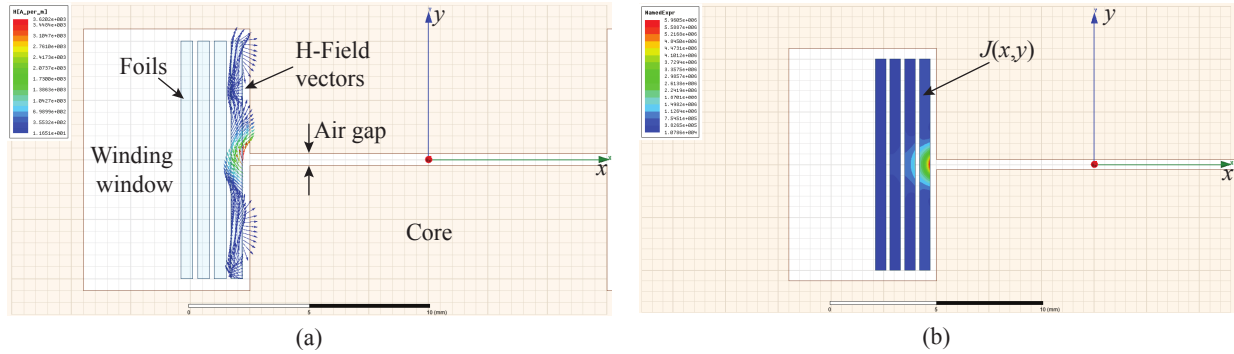


Figure 1: 2D FEM model of an inductor built on a gapped E-core with foil windings illustrating (a) non-homogeneous H-field distribution within the foil closest to the air gap and (b) non-uniform current distribution $J(x,y)$ in the foils (only one winding window is presented).

field, which influences the current distribution within the conductor itself (skin effect), and on the current distribution of the surrounding conductors (proximity effect). Foil winding loss calculations are typically converted into one-dimensional (1D) or two-dimensional (2D) models, where all magnetic field contributions of the conductors and air gaps need to be considered.

In the literature, the 1D calculation methods of proximity effect losses in foil windings are mostly based on the Dowell method, as e.g. described in [2]. Here, the magnetic field \vec{H} at the position of the winding layers is assumed to have only a single non-zero field component tangential to the winding layers. A more accurate approach is to take into account both H-field components (2D field approach) that influence the current distribution on the actual cross-section of the windings, as shown in Fig. 1(a).

For 2D methods, the main difficulty arises with the calculation of the transversal magnetic field in the windings induced by the air gap. Specifically, the fringing field around the air gap penetrates the windings causing eddy currents that produce additional losses. Neglecting these losses introduces large calculation errors, which in turn can lead to poor designs. The 2D modeling of the fringing flux around the air gap represents the main difficulty for developing a general applicable analytic equation for foil winding losses. Therefore (semi-) numerical methods like FEM have to be applied for this calculation task, e.g. as presented in [3]. Nowadays, the 2D loss calculations are often integrated into overall optimization procedures, which is not straightforward with FEM-based software.

The calculation of losses based on 2D methods in solid round wires and Litz wire windings under the influence of non-homogeneous magnetic field distributions, as generated by air gap(s), was analyzed in [4, 5, 6] and [7], respectively. Foil windings can be used to achieve better thermal properties compared to solid round and Litz windings since they have a higher copper fill factor. However, due to their geometry, foil windings are highly exposed to the effect of the air gap fringing field. Hence, they exhibit worse AC properties caused by increased eddy current losses and a non-uniform current distribution in the winding layer cross-section area. In order to calculate the winding losses, the current distribution in foils has to be determined as illustrated in Fig. 1(b). Air-gapped magnetic components are often used for the design of PFC, resonant and flyback power converters to avoid core saturation and to achieve the specified inductance value. Therefore, the availability of a fast and accurate calculation method for the foil winding losses of air-gapped inductors and transformers is necessary.

State-of-the-art approaches for the calculation of the 2D current distribution within foil windings employ FEM solvers, which are time-consuming and not efficient enough for the overall design optimization. The existing analytical methods, however, are based on rough simplifications. For example in [2], all foils are unified into a solid conductor. This approach returns accurate results only up to a certain frequency; at higher frequencies it was shown that the eddy current distribution is not comparable to the case of separate foils. In [8], the foils were replaced by line current densities, assuming that the copper foil winding acts as a shield to the fringing field. The air gap was replaced by a line current density characterized by a sum of spacial Fourier harmonics. Both analytical approaches [2] and [8] assume that there are no additional conductors in the space between the core and the foil windings.

In [9] a new semi-numeric/analytic method was presented based on an iterative procedure to calculate the non-uniform foil winding current distribution. The authors showed a good agreement between simulations and measurement results. The proposed loss model is not restrictive with respect to the geometry of windings and air gap. However, the iteration procedure has to be performed for each frequency step, which is very time consuming. In this paper, a novel 2D calculation approach using the Partial Element Equivalent Circuit (PEEC)-based modeling methodology for the fast calculation of the losses in foil windings is introduced. In contrast to [9], the non-uniform current distribution in the windings is directly calculated, which enables a faster calculation over a wide frequency range.

A PEEC-based Method for Foil Winding Loss Modeling

The Partial Element Equivalent Circuit method is a numerical technique derived from the integral form of Maxwell's equations [10]. It allows the coupling between the field and circuit domains, and thus is generally very useful for solving electromagnetic problems. The PEEC method reduces 3D geometrical representations of conductors into a set of circuit elements: resistances, partial inductances and partial capacitances. The conductor resistances model ohmic losses, whereas magnetic effects are represented by a partial inductance matrix \mathbf{L} and partial capacitances can be used to model the electric field coupling between conductors. Thus, based on the actual connectivity of the conductors, the 3D geometry is finally represented as an electric circuit consisting of R , L , and C elements. This PEEC-based circuit is finally solved via the Kirchhoff's voltage and current laws in a matrix equation.

The model discretization of a 3D structure leads to a set of sub-conductors. Each sub-conductor is defined as a circuit cell carrying an initially unknown volume current between two nodes of unknown potentials. The PEEC system is solved for these currents and voltages represented by the vectors \mathbf{i} and \mathbf{v} , respectively. For simple cell geometries, as rectangular or cylindrical cells, R , L , and C elements can be calculated analytically. An RLC circuit is finally defined by a system matrix and can be solved for the currents and voltages of the conductors in frequency- or time-domain. A general PEEC system matrix in the frequency domain is represented by a matrix of the form

$$\begin{bmatrix} \mathbf{A} & -(\mathbf{R} + j\omega\mathbf{L}) \\ (j\omega\mathbf{P}^{-1} + \mathbf{Y}_L) & \mathbf{A}^T \end{bmatrix} \begin{bmatrix} \mathbf{v} \\ \mathbf{i} \end{bmatrix} = \begin{bmatrix} \mathbf{v}_S \\ \mathbf{i}_S \end{bmatrix}. \quad (1)$$

The matrix \mathbf{A} is the connectivity matrix defining the connections between the sub-conductors, \mathbf{R} is the resistance diagonal matrix, \mathbf{L} is the symmetric positive definite partial inductance matrix consisting of partial self inductances $L_{\text{self}i}$ on the matrix diagonal, and off-diagonal partial mutual inductances L_{mij} . The capacitance matrix \mathbf{C} ($=\mathbf{P}^{-1}$) is neglected in the remainder of this paper, since electric field couplings are not further considered. The admittance matrix \mathbf{Y}_L consists of matrix stamps of additional circuit elements connected between PEEC nodes, and the vectors \mathbf{i}_S and \mathbf{v}_S represent current and voltage sources for the model excitations [10].

The PEEC Method and 2D Modeling of Foil Windings

Besides the simplification of the geometry, reducing the modeling problem from 3D to 2D allows an efficient calculation of the core boundary influence on the winding current distribution similar to [4].

The 3D geometry of a foil winding is shown in Fig. 2(a). The first step from 3D to 2D in Fig. 2(b) is to assume the foil length l in z -direction to be large compared to the dimensions in x - and y -direction. Further, a rectangular foil of the dimensions w and h is discretized into a set of N smaller conductors of the area $\Delta A = \Delta w \cdot \Delta h$ carrying a current density J_{si} , $i = 1 \dots N$, as shown in Fig. 2(c). In the next step, resistances per unit length are used, and partial inductances for 2D will be derived. The 2D resistance per unit length of the i -th rectangular conductor is calculated as

$$R_{i2D} = \frac{R_i}{l} = \frac{1}{\sigma \cdot \Delta A}, \quad (2)$$

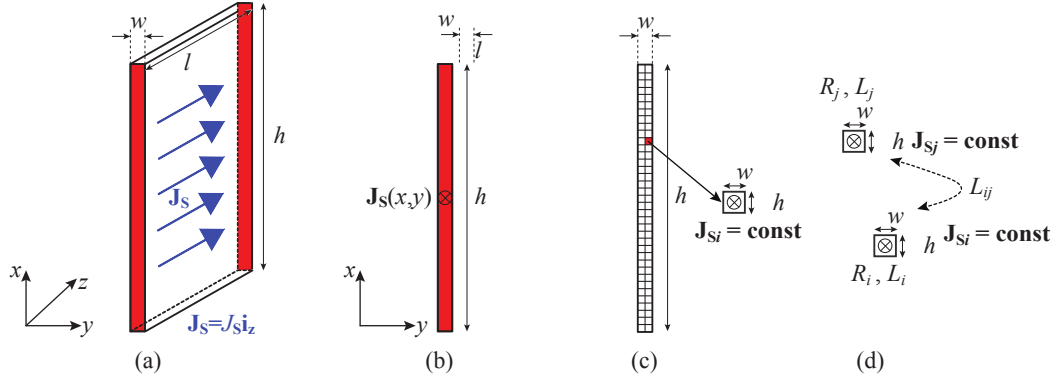


Figure 2: 2D PEEC modeling of a rectangular foil.

where σ is the electric conductivity and l is the length of the conductor. The partial self-inductance of a straight rectangular bar is calculated using equation (3) from [11],

$$L_{\text{self}} = L_i = \frac{\mu_0}{2\pi} \cdot l \cdot \left[\log\left(\frac{2 \cdot l}{R}\right) - 1 + \frac{R}{l} \right], \quad (3)$$

where l is the length of the conductor and R is the geometric mean distance [12] of the conductor cross section, marked with red colour in Fig. 2. Additionally, $l \gg R$ has to be fulfilled for (3) to be accurate. The 2D inductance formula given by (3) is then rewritten by applying $l \gg R$ ($l \rightarrow \infty$) as

$$L_{i2D} \approx \frac{\mu_0}{2\pi} \cdot [\log(2) + \log(l) - \log(R) - 1] = \frac{\mu_0}{2\pi} \cdot [\log(2) - 1] - \frac{\mu_0}{2\pi} \cdot \log(R) + \Delta L, \quad (4)$$

where $\Delta L = \frac{\mu_0}{2\pi} \cdot \log(l)$ denotes the only term in (4) depending on the length l . The expression ΔL makes the calculation of L_{i2D} and its application in equation (1) for 2D a non-trivial task, since ΔL diverges for $l \rightarrow \infty$. Descriptively, an inductor with infinite length has an infinite self inductance value per unit length. But, as shown later, the calculation of ΔL can be eliminated from the system matrix assuming $l \rightarrow \infty$ without any influence on the calculation results. The possibility to eliminate ΔL is plausible, since a solution of the 2D electromagnetic problem is well-defined and finally existing. The 2D mutual inductance between two parallel conductors with rectangular cross section as in Fig. 2(d) calculates as

$$L_{ij2D} = \frac{1}{w_1 h_1 w_2 h_2} \frac{1}{4} \cdot \sum_{i_1=0}^1 \sum_{k_1=0}^1 \sum_{i_2=0}^1 \sum_{k_2=0}^1 (-1)^{i_1+k_1+i_2+k_2} \cdot A_{i_1, k_1, i_2, k_2}^2 \cdot L_{\text{self}}(i_1, k_1, i_2, k_2), \quad (5)$$

which is based on the 3D formula for the mutual inductance given in [13]. Here, i_1, k_1, i_2 and k_2 represent the indices of the corners of two observed conductors with rectangular cross section, as shown in Fig. 3. According to (5), the 2D mutual inductance between two conductors can be interpreted as a sum of self-inductances of 16 conductors defined by the corners of two original conductors, as illustrated in Fig. 3. Other analytic formulations for a mutual inductance calculation of rectangular cells can be found in the literature [10]. However, (5) seems to give more accurate and numeric stable results for the 2D application, especially when the used sub-cell sizes differ significantly in their dimensions. Finally, (5) results in a weighted sum and application of the self-inductance formula (4) in two dimensions. After some calculations, it can be shown that the sum of weighting factors in (5) is equal to

$$\sum_{i_1=0}^1 \sum_{k_1=0}^1 \sum_{i_2=0}^1 \sum_{k_2=0}^1 (-1)^{i_1+k_1+i_2+k_2} \cdot A_{i_1, k_1, i_2, k_2}^2 = 4 \cdot w_1 h_1 w_2 h_2, \quad (6)$$

so that the following expression holds for the 2D mutual inductance (5)

$$L_{ij2D} = \Delta L + \frac{1}{w_1 h_1 w_2 h_2} \frac{1}{4} \cdot \sum_{i_1=0}^1 \sum_{k_1=0}^1 \sum_{i_2=0}^1 \sum_{k_2=0}^1 (-1)^{i_1+k_1+i_2+k_2} \cdot A_{i_1, k_1, i_2, k_2}^2 \cdot [L_{\text{self}}(i_1, k_1, i_2, k_2) - \Delta L]. \quad (7)$$

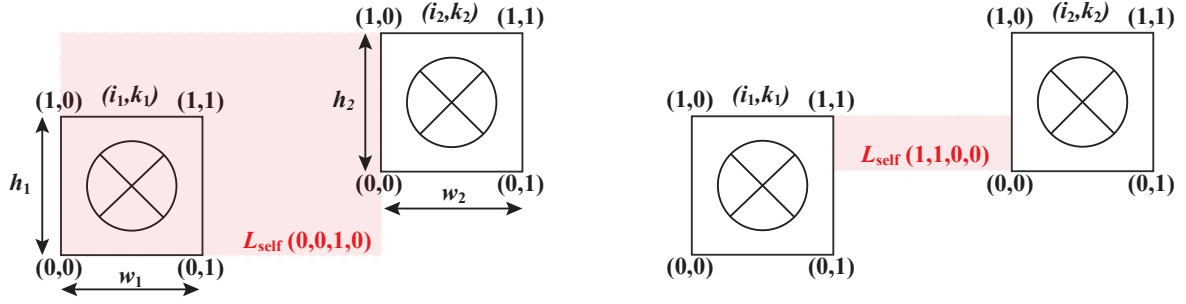


Figure 3: Calculation of the mutual inductance between two parallel conductors with rectangular cross section.

The remaining problem of the divergence of $\Delta L = \frac{\mu_0}{2\pi} \cdot \log(l)$ can now be eliminated. By assuming that the length l of all foils is the same, and since the mutual inductance calculation (7) is based on a weighted sum of self inductance calculations (4), then the limit $l \rightarrow \infty$ is nothing else than adding a matrix with identical (constant) entries $\Delta \mathbf{L} = [\frac{\mu_0}{2\pi} \cdot \log(l)]_{ij}$ to the inductance matrix \mathbf{L} . By a simple reasoning, it becomes clear that the constant Matrix $\Delta \mathbf{L}$ can be subtracted from the 2D inductance matrix in the system equation (1). This subtraction has finally no effect on the calculated current distribution, since only PEEC node potential *differences* determine the current distributions in the PEEC cells, and not their absolute value. Similarly, partial inductances are mathematically useful for the PEEC approach, but only loop inductances of a geometrically closed current loop have a valid physical interpretation. The loop inductance is not altered by adding a constant value to the inductance matrix. This fact can also be validated with a minimalistic 2-cell PEEC model example. Finally, the 2D PEEC system matrix (1) can be evaluated in the limit $l \rightarrow \infty$ and results in

$$\begin{bmatrix} \mathbf{A} & -(\mathbf{R}_{2D} + j\omega(\mathbf{L}_{2D} - \Delta \mathbf{L})) \\ \mathbf{0} & \mathbf{A}^T \end{bmatrix} \begin{bmatrix} \mathbf{v} \\ \mathbf{i} \end{bmatrix} = \begin{bmatrix} \mathbf{0} \\ \mathbf{i}_S \end{bmatrix}. \quad (8)$$

Here, \mathbf{A} is the $N_{\text{tot}} \times N_{\text{foil}}$ connectivity matrix that assures the sum of the currents of all foil sub-conductors to be equal to the total excitation current of the foil. The vector \mathbf{i}_S represents the model excitation current sources.

2D Modeling of Losses in the Presence of an Air Gap

For the complete modeling of losses in gapped magnetic inductors, the influence of the fringing field around an air gap and the influence of the magnetic core have to be taken into account.

Modeling the Magnetic Core Boundary

The influence of the core boundary is modeled via the mirroring method, similar as described in [1]. In particular, new additional virtual currents that are the mirrored version of the original currents need to be considered for modeling the influence of the magnetic material to the total magnetic field in the winding window. The magnetic field lines are ensured to enter perpendicular to the magnetic material boundary, thus an infinite core permeability is assumed, see Fig. 4(a). The addition of mirror currents to the PEEC model is simply performed by adding additional mutual inductances of the mirrored PEEC cells to the 2D inductance matrix \mathbf{L}_{2D} in (8). For instance, for a 2-cell PEEC model with a single mirror plane as shown in Fig. 4(b), the resulting inductance matrix is

$$\mathbf{L}^* = \mathbf{L}_{2D} + \mathbf{L}_{\text{mirror}} = \begin{bmatrix} L_{ii} & L_{ij} \\ L_{ij} & L_{jj} \end{bmatrix} + \begin{bmatrix} L_{in} & L_{im} \\ L_{im} & L_{jm} \end{bmatrix}. \quad (9)$$

The inductance matrix is symmetric, i.e. $L_{im} = L_{jn}$ in (9) applies. Since this approach is not introducing new variables into the PEEC model, the system matrix size is not changed and the matrix solution complexity does not increase with the number of introduced mirror planes. The computational overhead to include cell mirroring is solely the calculation of additional inductances between the original cells and their mirrored counterparts; the previously derived analytic expression (7) can be reused here.

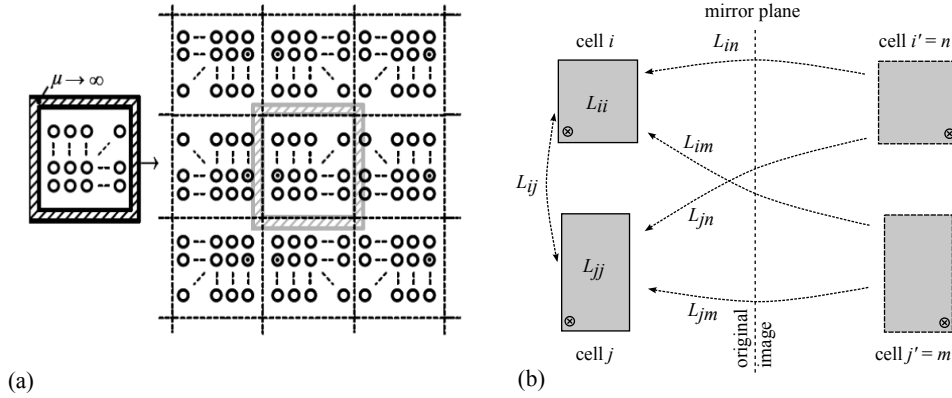


Figure 4: a) Illustration of the mirroring method to model the influence of the magnetic core material with the assumption $\mu \rightarrow \infty$. In case the 2D model is surrounded with permeable material, multiple mirror images can be used for increasing the calculation accuracy. The mirroring approach applied with the PEEC approach b) results in a modified inductance matrix.

Air Gap Modeling

The air gap is finally modeled as a fictitious conductor at the air gap position carrying the current equal to the magneto-motive force across the air gap [4]. The influence of the core and the air gap(s) is thus completely modeled via imaginary conductors. The air gap current has to be considered in the mirroring procedure, too. The accuracy of the presented approach is based on two assumptions: (1) the length of the air gap is small compared to the distance between the winding and the gap (which allows to replace the gap by a conductor) and (2) the relative permeability of the core is very high ($\mu_r \gg 1$), implying that the field lines are perpendicular to the walls of the core which allows the usage of the mirroring technique.

Foil Loss Modeling: 2D PEEC Method vs. 2D FEM

The 2D PEEC-based calculation of the winding losses is first verified by a 2D FEM simulation of an E-core inductor with the foil winding of four turns, as illustrated in Fig. 5. The 2D FEM simulation is performed using the software tool ANSYS Maxwell2D v16. The 2D PEEC simulation of the non-uniform current density distribution $J_{PEEC}(x, y)$ within the foils is shown in Fig. 6(a).

The 2D PEEC simulation of $J(x, y)$ is verified by the 2D FEM simulation comparing the calculated $J_{FEM}(x, y)$ and $J_{PEEC}(x, y)$ for $x = x_1$ and $x = x_2$ defined by two field probe lines through the first foil closest to the gap. Good matching between the 2D PEEC and the 2D FEM simulations is shown in Fig.

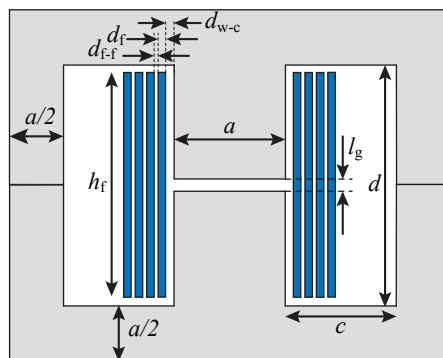


Figure 5: Example of an E-core inductor with a foil winding of 4 turns built on a high permeability core: $a = 15$ mm, $c = 7$ mm, $d = 11$ mm, $l_g = 0.5$ mm, $d_{w-c} = 0.3$ mm, $d_{f-f} = 0.2$ mm, $d_f = 0.5$ mm, $h_f = 10$ mm.

Table I: 2D PEEC-based vs. 2D FEM calculation of winding losses for the inductor in Figure 5.

	P_{PEEC} [mW/mm]	P_{FEM} [mW/mm]
Foil 1	69.077	69.353
Foil 2	10.461	10.259
Foil 3	3.140	3.110
Foil 4	2.086	2.077
Total	84.69	84.799
Rel. error		-0.12 %

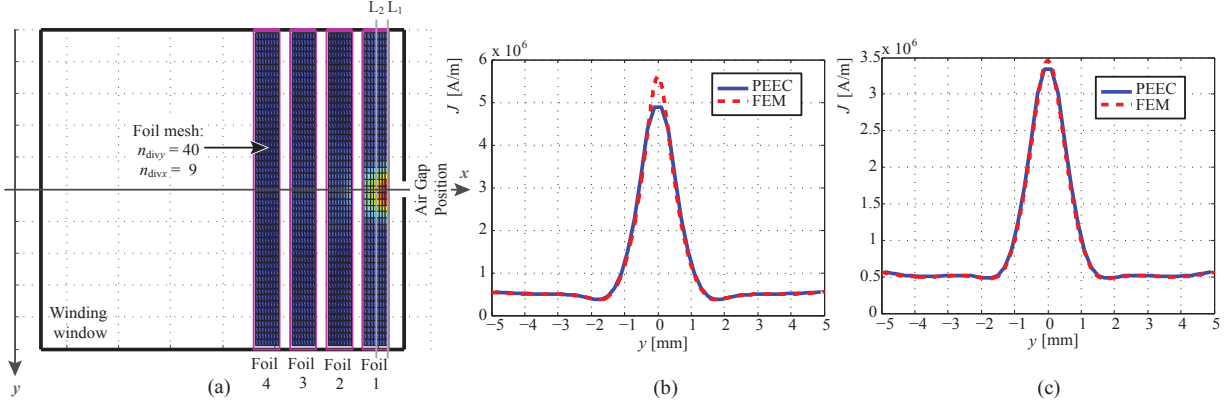


Figure 6: (a) Current density in the winding calculated based on the proposed 2D PEEC method. (b) Comparison between the 2D PEEC and 2D FEM simulations for the current density along (b) line $x = x_1$ (L1) and (c) line $x = x_2$ (L2) passing through the first foil closest to the air gap.

6(b) and (c). For the line $x = x_1$ closer to the gap, the maximum mismatch between two simulations is about 8% for the points in proximity to the air gap. Possible reasons for this deviation are inaccuracies due to the virtual conductor air gap model, discretization errors or the influence of the finite core permeability, since we assume $\mu_r \rightarrow \infty$. However, an agreement of 0.12% between the total power losses in four foils calculated via 2D PEEC and FEM is achieved, see Table I. A refined discretization of 40×9 sub-conductors is used for the first foil that is the most exposed to the fringing field, while the other three foils are discretized by 20×9 sub-conductors. The 2D PEEC simulation time of the given example was around 10s, while for the 2D FEM simulation using ANSYS Maxwell2D v16, a simulation time of 1 min was required.

Experimental Verification

The proposed 2D PEEC approach was implemented in the software tool GeckoMAGNETICS [14], which is further used to calculate the total losses of an actual E-core inductor with foil windings. In the following sections, the software GeckoMAGNETICS and the experimental verification setup are presented. The specifications of the modeled inductor, as shown in Fig. 7(a), are given in Table II.

Table II: Inductor specifications for the experimental verification.

Core material	Ferrite (EPCOS N87)
Core size	$3 \times \text{E42/21/15}$ E-core sets (stacked)
Air gap length [mm]	3.18
Winding type	Copper foil winding, 20 turns
Winding size [mm]	$d_f = 0.1$, $h_f = 25$, $d_{f-f} = 0.165$, $d_{w-c} = 1.05$
DC resistance	$20.8 \text{ m}\Omega$ @ $T_{\text{wind}} = 23^\circ \text{C}$

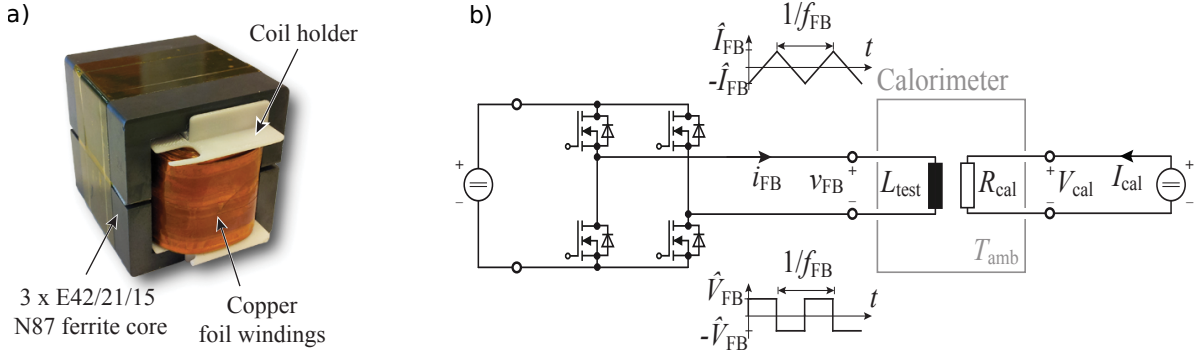


Figure 7: a) Photo of the inductor used for the experimental verification of the developed PEEC-based approach for the calculation of foil winding losses. b) Measurement setup with a full bridge converter that is used to excite the inductor under test, with a triangular current. After reaching the setpoint-dependent steady-state ambient temperature $T_{amb,ss}$ inside of the calorimeter, the full bridge is turned off while turning on the calibration circuit. Adjusting $P_{cal} = I_{cal}V_{cal}$ in order to keep the calorimeter ambient temperature constant at $T_{amb,ss}$ yields a good measure of the total inductor losses, i.e., $P_{L_{test}} \approx P_{cal}$.

GeckoMAGNETICS

GeckoMAGNETICS [14] enables fast and accurate modeling of inductive power components, such as inductors and transformers, in a user-friendly way. As input, the winding properties, core material data, current and voltage waveforms and thermal properties have to be specified. The software enables to separately evaluate core losses and winding losses of the inductor design. Additionally, it allows to optimize the design towards either lower power losses or lower inductor volume, for instance by selecting a different core material, or using a different winding geometry. GeckoMAGNETICS employs the loss map approach described in [15] for the calculation of the core losses. For the calculation of the total winding losses, the foil sections inside the winding window and perpendicular to it are distinguished and calculated separately via 2D models. The varying lengths of the winding turns within the winding stack are considered so that the innermost turn is the shortest.

Measurement Setup

The inductor loss measurement setup shown in Fig. 7 was used in order to experimentally verify the PEEC-based approach. The setup consists of a full bridge converter and a calorimeter containing the inductor L_{test} under test, and a resistor R_{cal} for the loss calibration. The calorimeter is further equipped with a fan to achieve a homogeneous air temperature inside the box as well as various temperature sensors for measuring the ambient, the core and the winding temperatures, T_{amb} , T_c and T_{wind} , respectively. A two-step measurement approach is applied for each operating point.

In a first step, the full bridge converter is used to excite L_{test} with a rectangular voltage waveform, leading to a triangular current. Eventually, this will heat up the calorimeter to the steady-state ambient temperature $T_{amb,ss}$, which depends on the operating point.

In a second step, the full bridge is turned off while turning on the calibration circuit. The inductor losses can now be estimated by adjusting $P_{cal} = I_{cal}V_{cal}$ so as to keep the calorimeter ambient temperature constant at $T_{amb,ss}$. Ideally, this requires $P_{cal} = P_{L_{test}}$.

As the setup of the calorimeter remains unchanged between step (i) and (ii), the losses of the fan and the temperature sensors are not relevant. The DC values I_{cal} and V_{cal} are measured with high-precision equipment, while \hat{i}_{FB} and \hat{v}_{FB} are measured with standard oscilloscope probes. A DC blocking capacitor in series to L_{test} was not required as the measured DC component of i_{FB} was negligible in all measurements.

GeckoMAGNETICS Simulation vs. Measurements

The measurements were performed for three operating points, as specified in Table III. The comparison between the corresponding measurements and the results from GeckoMAGNETICS is summarized in

Table III: Specifications of three measured operating points (OP) and comparison between measurements and GeckoMAGNETICS simulations of total inductor losses.

OP	OP Specifications			GeckoMAGNETICS			Measurements	Rel. Err.
	f_{FB} [kHz]	\hat{V}_{FB} [V]	\hat{I}_{FB} [A]	P_{wind} [W]	P_{core} [W]	P_{tot} [W]	P_{tot} [W]	[%]
1	5	25.87	10.73	3.785	0.284	4.069	4.328	-5.98
2	15	50.73	7.13	3.492	0.395	3.887	3.783	2.73
3	30	69.84	4.94	2.60	0.371	2.939	2.565	15.96

Table III. As the calorimetric measurement method does not allow distinguishing between core and winding losses, the employed inductor is therefore designed for the purpose to verify the proposed winding loss model. In particular, according to the simulation results of the analysed inductor example, the winding losses contribute the dominating loss component for all measured operating points. The core loss measurement errors have a low impact on the total inductor losses, see Fig. 8. The maximum difference between the measurements and the GeckoMAGNETICS modeling results of less than 16%. The error source for the 16% error at 30 kHz is difficult to detect. Possible reasons could be modeling issues of the 2D geometry simplification, the simplified GeckoMAGNETICS thermal model that assumes homogeneous temperatures of the core and the winding, the accuracy of the loss-map approach for the calculation of core losses using EPCOS N87 ferrite material datasheets properties, and/or the precision of the calorimetric measurement setup defined by reaching the steady-state $T_{amb,ss}$ level. The simulation time for an operating point is of the order of several seconds. Accordingly, the presented verification shows that GeckoMAGNETICS, with the implemented 2D PEEC-based modeling approach, can be used for the efficient calculation of foil winding losses, and hence, for an overall design of gapped E-core inductors built with foil windings with an acceptable engineering accuracy. The screenshots of the GeckoMAGNETICS results are presented in Fig. 8 showing the non-uniform loss distribution across the foils due the air gaps and the shares of loss components, respectively.

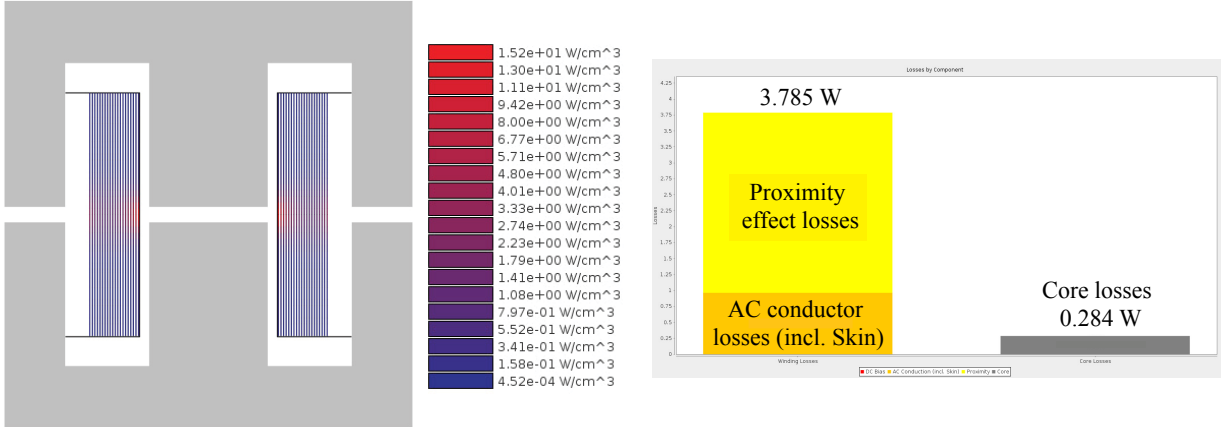


Figure 8: GeckoMAGNETICS simulation results for the first operating point (OP₁): Visualization of the non-uniform loss distribution across the foils due the air gap and the origin of total loss distribution.

Summary and Conclusion

This paper presents a new 2D approach for the fast and accurate calculation of foil winding losses taking into account the skin and proximity effects and the influence of the air gap fringing field. The proposed PEEC-based approach was compared and validated with 2D FEM simulations; a good level of accuracy was achieved with a fast computation time. The developed approach was implemented in the software GeckoMAGNETICS which enables the calculation of the total inductor losses, i.e. including both core and winding losses. Additionally, the simulation result of a gapped E-core foil winding inductor was successfully verified by measurements using a calorimetric measurement setup. This new 2D approach

thus allows optimizing complete inductor designs with foil windings towards minimum losses and/or minimum inductor volumes in an efficient and accurate way.

The comparison between experimental results and simulations in this paper revealed that the E-core air gap reluctance calculation has to be revised in the case of the foil windings. Specifically, the effective cross-sectional area of the air gap calculated by using the Schwarz-Christoffel transformation leads to an increased inductance value L_{calc} in comparison to the measured inductance, L_{meas} , e.g., $L_{\text{calc}} = 138\ \mu\text{H}$ and $L_{\text{meas}} \approx 120\ \mu\text{H}$. This can be explained by the electromagnetic effect of foils acting as a shield to the air gap fringing field.

In future research, the calculation accuracy and speed of the new 2D approach could be further improved by an adaptive PEEC meshing. Furthermore, considering capacitive effects would be necessary to generate valid high frequency inductor models.

References

- [1] J. Muhlethaler, M. Schweizer, R. Blattmann, J. Kolar, and A. Ecklebe, "Optimal design of LCL harmonic filters for three-phase PFC rectifiers," *IEEE Trans. Power Electron.*, vol. 28, no. 7, pp. 3114–3125, 2013.
- [2] P. Wallmeier, "Improved analytical modeling of conductive losses in gapped high-frequency inductors," *IEEE Trans. Ind. Appl.*, vol. 37, no. 4, pp. 1045–1054, 2001.
- [3] F. Robert, P. Mathys, and J. P. Schauwers, "A closed-form formula for 2D ohmic losses calculation in SMPS transformer foils," in *Proc. of the 14th App. Power Electronics Conf. (APEC)*, vol. 1, 1999, pp. 199–205.
- [4] V. Valche and A. Van den Bossche, *Inductors and transformers for power electronics*. CRC Press, 2005.
- [5] F. Holguin, R. Prieto, R. Asensi, and J. Cobos, "Power losses calculations in windings of gapped magnetic components," in *Proc. of the 29th Appl. Power Electronics Conf. and Exp. (APEC)*, 2014, pp. 2605–2506.
- [6] C. Wei and J. Zheng, "Improved winding loss theoretical calculation of magnetic component with air-gap," in *Proc. of the 7th Int. Power Electronics and Motion Control Conf. (IPEMC)*, vol. 1, 2012, pp. 471–475.
- [7] A. Stadler and C. Gulden, "Copper losses of litz-wire windings due to an air gap," in *Proc. of the 15th European Conference on Power Electronics and Applications (EPE)*, 2013, pp. 1–5.
- [8] A. Van den Bossche and V. Valchev, "Eddy current losses and inductance of gapped foil inductors," in *Proc. of the 28th Annual Conference of the Industrial Electronics Society (IECON)*, vol. 2, 2002, pp. 1190–1195.
- [9] D. Leuenberger and J. Biela, "Semi-numerical method for loss-calculation in foil-windings exposed to an air-gap field," in *Proc. of International Power Electronics Conference (IPEC-ECCE-ASIA)*, 2014, pp. 868–875.
- [10] A. E. Ruehli, "Equivalent circuit models for three dimensional multiconductor systems," *IEEE Trans. Microw. Theory Tech.*, vol. 22, no. 3, pp. 216–221, 1974.
- [11] E. Rosa, "The self and mutual inductance of linear conductors," *Bulletin of the National Bureau of Standards*, pp. 301–344, 1908.
- [12] P. C. Magnusson, "Geometric mean distances of angle-shaped conductors," *Trans. of the American Inst. of Electrical Engineers*, vol. 70, no. 1, pp. 121–123, 1951.
- [13] G. Zhong and C.-K. Koh, "Exact closed-form formula for partial mutual inductances of rectangular conductors," *IEEE Trans. Circuits Syst. I*, vol. 50, no. 10, pp. 1349–1352, 2003.
- [14] (2015). [Online]. Available: <http://www.gecko-simulations.com/>
- [15] J. Muhlethaler, J. Biela, J. Kolar, and A. Ecklebe, "Improved core-loss calculation for magnetic components employed in power electronic systems," *IEEE Trans. on Power Electronics*, vol. 27, no. 2, pp. 964–973, 2012.